

A DOUBLY LATENT SPACE JOINT MODEL FOR LOCAL ITEM AND PERSON DEPENDENCE: AN APPLICATION TO COMPETENCE PROFILE TEST OF VERBAL DEDUCTIVE REASONING

BY ICK HOON JIN^{*} AND MINJEONG JEON[†]

University of Notre Dame^{} and University of California, Los Angeles[†]*

We develop a new analytic approach for binary item response data, specifically the data come from the Competence Profile Test of Deductive Reasoning - Verbal (DRV). The analysis of the DRV test data is challenging due to its unknown local item and local person dependence structures, which cannot be properly performed with current methodologies. Our innovation is to propose a new latent space joint modeling idea that can manage item dependence and person dependence structures from person network views and item network views, respectively. Our model estimates relative distances between pairs of items and relative distances between pairs of persons, which in turn are used to describe item and person dependence structures. The proposed approach was successfully applied to analyze the DRV test data. Our analysis results revealed that the DRV data included three person clusters and four item clusters.

1. Introduction. The Competence Profile Test of Deductive Reasoning - Verbal (DRV; [Spiel, Gluck and Gossler, 2001](#); [Spiel and Gluck, 2008](#)) was developed based on Piaget's cognitive developmental theory ([Piaget, 1971](#)) for the purpose of evaluating children's cognitive developmental stages based on their deductive reasoning levels and profiles. According to Piaget's theory, children move through four qualitatively different cognitive developmental stages: the sensorimotor, the preoperational, the concrete-operational, and the formal-operational stages. The progress from one stage to another requires children to apply a major reorganization of their thinking process ([Draney et al., 2007](#)). For instance, children in the concrete-operational stage are expected to perform logical operations only on concrete objects. Children in the formal-operational stage are expected to perform logical operations on abstractions as well as concrete objects. The DRV test focuses on identifying children in these two developmental stages.

The 24 DRV test items are characterized with the following design factors:

Keywords and phrases: Latent Space Model, Multiplex Network, Item Response Model, Local Dependence, Cognitive Assessment

1. Type of inference: Modus Ponens (MP), Modus Tollens (MT), Affirmation of Consequent (AC), and Negation of Antecedent (NA)
2. Content of the conditional: Concrete (CO), Abstract (AB), and Counterfactual (CF)
3. Presentation of the antecedent: no negation (NN) and Negation (NE).

First, items are classified by the type of inference into four types: (1) Modus Ponens (A, therefore B), (2) Negation of Antecedent (Not A, therefore B or not B), (3) Affirmation of Consequent (B, therefore A or not A), and (4) Modus Tollens (Not B, therefore not A). Modus ponens (MP) and modus tollens (MT) involve biconditional conclusions; therefore, the response to those items is either “yes” or “no”. For negation of antecedent (NA) and affirmation of consequent (AC), the correct solution is “perhaps” because the premise does not allow for deciding whether these conclusions are correct. NA and AC are called logical fallacies because they provoke a biconditional choice, but a logically incorrect conclusion (“no” for NA, “yes” for AC). Second, items are categorized by the content of the conditional into three groups: concrete (CO), abstract (AB), and counterfactual (CF) contents. For example, a counterfactual content item is “If an object is put into boiling water, it becomes cold”. Third, items are characterized by the mode of presentation of the antecedent: the antecedent presented with negation (NE, e.g., “if the sun does not shine, Peter wears blue pants”) or without negation (NN, e.g., “if the sun shines, Tina wears a red skirt”). Table 1 lists example items that correspond to the four inference types that show concrete content (CO) and no negation (NN) features.

TABLE 1

Example DRV items that correspond to four types of inference with concrete content (CO) and no negation (NN). The premise is “If Tom is ill, he is lying in his bed.”

Type of inference	Item	Correct solution
Modus Ponens (MP)	Tom is ill. Is Tom lying in his bed?	Yes
Modus Tollens (MT)	Tom is not lying in his bed. Is Tom ill?	No
Negation of Antecedent (NA)	Tom is not ill. Is Tom lying in his bed?	Perhaps
Affirmation of Consequent (AC)	Tom is lying in his bed. Is Tom ill?	Perhaps

Source: [Draney et al. \(2007\)](#)

Research has shown that children at the concrete-operational stage can treat all four inferences as biconditional (e.g., [Evans, Newstead and Byrne,](#)

1993; Janveau-Brennan and Markovits, 1999). As cognitive development progresses, the performance on fallacy items (NA, AC) usually improves, but the performance on biconditional items (MT and MP) may become worse because children who notice the uncertainty of the fallacies tend to over-generalize (e.g., Byrnes and Overton, 1986; Markovits et al., 1998). Other research discussed that concrete items are easier than abstract and counterfactual items. In addition, when negation is included in the antecedents, items reportedly become more difficult (e.g., Roberge and Mason, 1978). On the other hand, it is unclear whether there are difficulty differences between abstract and counterfactual items (e.g., Overton, 1985).

Researchers have applied finite-mixture item response theory (IRT) models to the DRV data (Spiel, Gluck and Gossler, 2001; Draney et al., 2007). Finite-mixture IRT models, while they can identify clustering among people, still require local independence of people within cluster. Hence, finite-mixture models cannot handle additional person dependence within cluster generated due to the potential similarities in their response patterns. When the independence assumption for respondents is violated, however, statistical inference for the model parameters are likely to be biased (e.g., Fox and Glas, 2001).

In addition, mixture IRT models rely on local item independence which is a critical assumption in IRT analysis. Local item independence can be defined as:

$$P(X_{ki} = 1, X_{kj} = 1 | \theta_k) = P(X_{ki} = 1 | \theta_k) \times P(X_{kj} = 1 | \theta_k),$$

where X_{ki} and X_{kj} are a pair of binary responses for item i and j ($i \neq j$) for person k and θ_k is person k 's latent trait.

As discussed above, the design of the DRV test is likely to generate a local dependence structure across items that share the same test design features. Violations of the local item independence assumption can severely distort the item and person parameter estimates as well as test information functions (e.g., Chen and Thissen, 1997; Liu and Maydeu-Olivares, 2012). At present, there seems to be no method available to manage unknown local item dependence structures. As an alternative method, researchers attempted to detect the presence of local item dependence prior to main item analysis. However, identifying local item independence violations is generally a challenging task (Liu and Maydeu-Olivares, 2012).

The purpose of the current study is to propose a new item analytic method to address the local dependence structure of the DRV data. Our key idea is to adapt a latent space modeling approach, which is typically used for network data analysis, in the context of analyzing item response data. Our proposed

approach captures the dependence structure of items from person network views as well as the dependence structure of people from item network views.

The contributions of our study can be summarized as follows: First, we develop an item analysis strategy that solves local item dependence and person dependence problems without needing a priori local dependence structures. Existing approaches usually require known dependence structures at the person and item sides. Second, our proposed approach offers an additional benefit by providing the dependence/cluster structure of the items and persons, while simultaneously estimating item and person parameter estimates. Note that to investigate local dependence structures of item response data, a two-step procedure is usually needed, first to fit an IRT model (step 1) and then to compute the test statistics (step 2). If a violation is found, the model parameter estimates obtained from step 1 are likely inaccurate. In contrast, our approach offers a single step procedure where item and person parameters are accurately estimated as well as local item and person dependence structures. Third, our model is a novel application of a latent space model. In addition, we expand an existing latent space model into a doubly latent space joint model for the purpose of simultaneously capturing item network and person network. Finally, our approach can be generally utilized to analyze other binary item response data, although the development of our method was motivated by the DRV test data analysis. Our method can also be applied to develop statistical indices to evaluate local dependence among items and among people, which can be useful for test construction, test validation, and scoring purposes.

We organize the remainder of this article as follows. In Section 2, we describe our proposed doubly latent space joint model for the analysis of item response data. We present the MCMC computational framework in Section 3. In Section 4, we provide an illustrative example. In Section 5, we apply our proposed approach to analyze the DRV data and to describe the dependence structures of items and persons. We provide our conclusion and discussion on future developments in Section 6.

2. Doubly Latent Space Joint Model for the Analysis of Item Response Data.

2.1. *Latent Space Model.* Statistical analysis based on a latent Euclidean space has been a useful tool for the analysis of data in the form of dissimilarities. [Oh and Raftery \(2001\)](#) makes exact inference about latent space and provides a principled property for determining the dimension of latent space. Their work has been extended to the model-based network data analysis, which inherently includes dependent structures within data ([Hoff, Raftery](#)

and Handcock, 2002).

Assume that each node i has an unknown position \mathbf{z}_i in a D -dimensional Euclidean latent space. A latent space model (Hoff, Raftery and Handcock, 2002; LSM) introduces the distance between the latent position of \mathbf{z}_i as a penalty in a logistic regression framework to consider interactions between nodes. Then, the probability of a link between the pairs of nodes depends on the distance between them. Generally, the smaller the distance between two nodes in the latent space, the greater the probability that they connect.

Let N be the number of nodes in networks and Y be the $N \times N$ adjacency matrix containing the network information, where $y_{ij} = 1$ when node i and j are connected and 0 otherwise. The diagonal terms, $y_{ii} = 0$ unless node i is self-connected. Let Z be an $N \times D$ latent position matrix where each row $\mathbf{z}_i = (z_{i1}, \dots, z_{iD})$ is the D -dimensional vector indicating the position of node i in the D -dimensional Euclidean space. The LSM can be written by

$$(2.1) \quad P(\mathbf{Y} \mid \mathbf{Z}, \beta, \gamma) = \prod_{i \neq j} P(y_{ij} \mid \mathbf{z}_i, \mathbf{z}_j, \beta, \gamma) = \prod_{i \neq j} \frac{\exp(\beta - \|\mathbf{z}_i - \mathbf{z}_j\|)^{y_{ij}}}{1 + \exp(\beta - \|\mathbf{z}_i - \mathbf{z}_j\|)},$$

where $\|\mathbf{z}_i - \mathbf{z}_j\| = \sqrt{\sum_{d=1}^D (z_{id} - z_{jd})^2}$ is an Euclidean distance between nodes i and j . The number of dimension D is often chosen as 2 or 3 for display reasons. To estimate the intercept β and the latent positions Z , a Bayesian approach is typically applied. We assume that the \mathbf{z}_i are independent draws from a spherical multivariate normal distribution, so that

$$\mathbf{z}_k \stackrel{iid}{\sim} \text{MVN}_d(0, \sigma_z^2 I_d).$$

Refer to Hoff, Raftery and Handcock, 2002; Handcock, Raftery and Tantrum, 2007; Krivitsky et al., 2009; Raftery et al., 2012; Rastelli, Friel and Raftery, 2015 for more details on the latent space model.

The motivation for LSM is similar to that for multidimensional scaling (Breiger, Boorman and Arabie, 1975; Davison, 1983; MDS), which is a class of methods that spatially represents observations based on similarity and dissimilarity measures between sample pairs. However, how each method works is different between LSM and MDS; LSM provides a visual and interpretable model-based spatial representation of interactions among individuals based on latent locations, while MDS primarily uses a data-analytic means of dissimilarity, which is chosen in an ad-hoc manner.

Distances between Euclidean latent spaces are invariant under rotation, reflection, and translation (Hoff, Raftery and Handcock, 2002; Shortreed,

Handcock and Hoff, 2006). Thus, for each latent position matrix Z , there are an infinite number of other possible positions that result in the same log-likelihoods. This invariance property of a latent space can cause two major problems in the parameter estimation of latent space models. First, because the model specifies distances between actors, the estimated latent position of actors may poorly represent the actual actor positions, even though the distances between actors may be accurately determined. Second, this invariant property prompts the unstable mixing of Markov chain Monte Carlo (MCMC) for latent spaces of low-degree nodes, causing the overestimation of a variability of the latent positions. Currently, there are no established solutions to these problems. To address those issues, we will work with distance measures between latent spaces rather than latent positions themselves. To handle the variance overestimation issue, we will fix the variance parameter of \mathbf{z}_i based on the reasoning that the variance of \mathbf{z}_i can be seen as a nuisance given that the purpose of LSM is to project the latent features of nodes into Euclidean spaces.

2.2. *Latent Space Joint Model for Item Response Data Analysis.* Suppose $X_{n \times p}$ is an item response dataset where n is the number of respondents, p is the number of items, and x_{ki} indicates a binary response to item i for person k . To apply a latent space model to the item response data, we first need to construct two sets of adjacency matrices, $Y_{i, n \times n}$ for item i and $U_{k, p \times p}$ for person k :

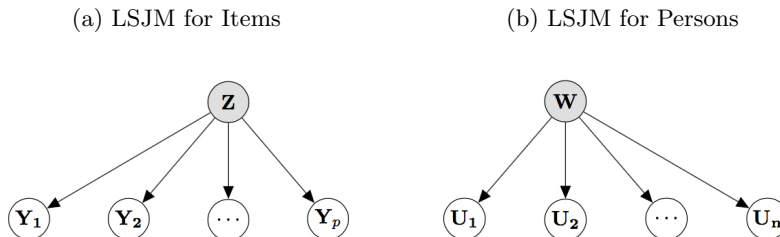
$$(2.2) \quad Y_{i, n \times n} = \{y_{i, kl}\} = \{x_{ki}x_{li}\} \quad \text{and} \quad U_{k, p \times p} = \{u_{k, ij}\} = \{x_{ki}x_{kj}\}.$$

Specifically, $y_{i, kl}$ takes 1 if persons k and l are related ($k \neq l$) and 0 otherwise for item i ($i = 1, \dots, p$); that is, $x_{ki}x_{li}$ indicates an interaction between person k and person l for item i . Similarly, $u_{k, ij} = 1$ if items i and k are correlated ($i \neq j$) and 0 otherwise for person k ($k = 1, \dots, n$) with $x_{ki}x_{kj}$ indicating an interaction between items i and j for person k .

It is noteworthy that there are p sets of adjacency matrices $Y_{i, n \times n}$ and n sets of adjacency matrices $U_{k, p \times p}$. Here $\mathbf{Y} = \{Y_i\}$ and $\mathbf{U} = \{U_k\}$ are the person network views and the item network views that are constructed to estimate item properties and person characteristics, respectively.

Since \mathbf{Y} and \mathbf{U} are multiplex networks (Mucha et al., 2010), the multiple individual networks needed to be integrated. To this end, we introduce a respective latent variable for the item network and person network, by adapting the latent space joint modeling (LSJM) approach (Gollini and Murphy, 2016). As the result, we obtain a respective latent space joint model for items and persons.

FIG 1. *Latent Space Joint Model for Items (a) and Latent Space Joint Model for Persons (b). $\mathbf{Z} = \{\mathbf{z}_k\}$ and $\mathbf{W} = \{\mathbf{w}_i\}$ denotes a latent space for Y_i and U_k , respectively, where $i = 1, \dots, p$ and $k = 1, \dots, n$. The latent space joint model for items contains n person latent spaces and the latent space joint model for persons includes p item latent spaces.*



In Fig 1, $\mathbf{Z} = \{\mathbf{z}_k\}$ and $\mathbf{W} = \{\mathbf{w}_i\}$ denote a continuous latent variable for person network Y_i for item i and item network U_k for person k , respectively. The multiple networks \mathbf{Y} are assumed to be conditionally independent given the latent space \mathbf{Z} where $\mathbf{z}_k \sim N(0, \sigma_z^2 I_D)$ is determined in a D -dimensional latent space and summarizes the latent feature information of nodes from all individual network views \mathbf{Y} . The LSJM for items illustrated in Figure 1(a) can be written as follows:

$$(2.3) \quad P(\mathbf{Y} | \mathbf{Z}, \boldsymbol{\beta}) = \prod_{i=1}^p P(Y_i | \mathbf{Z}; \beta_i) = \prod_{i=1}^p \prod_{k \neq l} \frac{\exp(\beta_i - \|\mathbf{z}_k - \mathbf{z}_l\|)^{y_{i,k,l}}}{1 + \exp(\beta_i - \|\mathbf{z}_k - \mathbf{z}_l\|)}$$

where β_i is the intercept parameter for item i , \mathbf{z}_k and \mathbf{z}_l indicate the latent positions for person k and person l . Here β_i can be interpreted as the (inverse logit transformed) probability of correctly answering item i when respondents k and l have the same latent space positions (in other words, when respondents k and l have the same ability levels). Note that β_i is conceptually similar to the item easiness parameter in the Rasch model; the key difference is that β_i in LSJM is determined by whether pairs of respondents, with similar or different abilities, jointly answer the item correctly. For instance, a large β_i is obtained when pairs of respondents with highly different abilities (or with a large distance in their latent space positions) tend to answer the item correctly. On the other hand, a small β_i is obtained when pairs of respondents fail to correctly answer the item together. In this sense, one can utilize the item intercept parameter estimates to discuss and compare the overall easiness levels of individual items.

The prior distributions for the model parameters are specified as $p(\beta_i) \sim N(0, \sigma_\beta^2)$, $\mathbf{z}_k \sim N(0, \sigma_z^2 I_D)$ with fixed σ_β^2 , σ_z^2 . As aforementioned, fixing

σ_z^2 can resolve the variance overestimation problem of LSJM. Then, the posterior distribution of β_i and the latent variable \mathbf{z}_k are specified as

$$(2.4) \quad \begin{aligned} \pi(\beta_i | Y_i, \mathbf{Z}) &\propto \pi(\beta_i) \prod_{k \neq l} \frac{\exp(\beta_i - \|\mathbf{z}_k - \mathbf{z}_l\|)^{y_{i,kl}}}{1 + \exp(\beta_i - \|\mathbf{z}_k - \mathbf{z}_l\|)} \\ \pi(\mathbf{z}_k | \mathbf{Y}, \boldsymbol{\beta}) &\propto \pi(\mathbf{z}_k) \prod_{i=1}^p p(Y_i | \mathbf{z}_k, \beta_i). \end{aligned}$$

Similarly, we assume the multiplex network \mathbf{U} are conditionally independent given the latent space \mathbf{W} with $\mathbf{w}_i \sim N(0, \sigma_w^2 I_D)$ is determined in a D -dimensional latent space that summarizes the latent feature information of the nodes from all individual network views \mathbf{U} . The LSJM for persons illustrated in Figure 1(b) can be written as follows:

$$(2.5) \quad P(\mathbf{U} | \mathbf{W}, \boldsymbol{\theta}) = \prod_{k=1}^n P(U_k | \mathbf{W}; \theta_k) = \prod_{k=1}^n \prod_{i \neq j} \frac{\exp(\theta_k - \|\mathbf{w}_i - \mathbf{w}_j\|)^{u_{k,ij}}}{1 + \exp(\theta_k - \|\mathbf{w}_i - \mathbf{w}_j\|)}$$

where θ_k is the person trait for person k , \mathbf{w}_i and \mathbf{w}_j indicate the latent positions for item i and item j . Here θ_k can be interpreted as the (inverse logit transformed) probability of correctly answering items i and j for person k when items i and j have the same latent space positions (in other words, when items i and j have the same intercept values). Note that θ_k is conceptually similar to the person ability parameter in the Rasch model; however, the key difference is that θ_k in LSJM is determined by whether the person correctly answer pairs of items with similar or different levels of easiness. For instance, a large θ_k is obtained when the respondent tends to answer pairs of items with highly different levels of easiness (or with a large distance in their latent space positions). A small θ_k is obtained when the person fails to answer many pairs of items correctly. That is, one can use the person intercept parameter estimates to compare the level of abilities (or latent traits) among people.

The prior distribution is specified for $p(\theta_k) \sim N(0, \sigma_\theta^2)$, $\mathbf{w}_i \sim N(0, \sigma_w^2 I_D)$ with fixed $\sigma_\theta^2, \sigma_w^2$. The posterior distribution of $\theta_1, \dots, \theta_n$ and the latent variable \mathbf{w}_i can then be specified as

$$(2.6) \quad \begin{aligned} \pi(\theta_k | U_k, \mathbf{W}) &\propto \pi(\theta_k) \prod_{i \neq j} \frac{\exp(\theta_k - \|\mathbf{w}_i - \mathbf{w}_j\|)^{u_{k,ij}}}{1 + \exp(\theta_k - \|\mathbf{w}_i - \mathbf{w}_j\|)}. \\ \pi(\mathbf{w}_i | \mathbf{U}, \boldsymbol{\theta}) &\propto \pi(\mathbf{w}_i) \prod_{k=1}^n p(U_k | \mathbf{w}_i, \theta_k). \end{aligned}$$

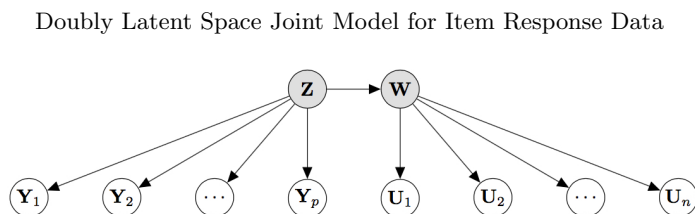
2.3. *Doubly Latent Space Joint Model for Item Response Data.* To simultaneously estimate the item intercept parameters from the person network view and the person intercept parameters from the item network view, a remaining task is to combine the two LSJM models (for person and item network views) constructed in Section 2.2. Unfortunately, the two latent space joint models cannot be combined directly because of the mismatch in the $\mathbf{Z}_{n \times n}$ and $\mathbf{W}_{p \times p}$ dimensions. To resolve this issue, we will make an assumption that the latent space of item i (\mathbf{w}_i) is a function of the latent spaces of all respondents (\mathbf{Z}), where the function is defined as follows:

$$(2.7) \quad \mathbf{w}_i = f_i(\mathbf{Z}) = \sum_{k=1}^n \frac{x_{ki}z_k}{\sum_{k=1}^n x_{ki}}.$$

That is, \mathbf{w}_i is an average of latent space collections for the respondents who give a correct answer to item i . Viewing one latent space as a weighted function of the other latent space makes sense because the two latent spaces (from person and item network views) are essentially determined based on a single item response dataset.

Based on this assumption, we can combine the two LSJM models for items and persons such that once \mathbf{Z} is estimated, \mathbf{w}_i is estimated without additional MCMC computation. We will refer to the resulting, integrated model as a doubly latent space joint model for item response data (DLSJM). Figure 2 illustrates the DLSJM.

FIG 2. *Doubly Latent Space Joint Model.* $\mathbf{Z} = \{\mathbf{z}_k\}$ and $\mathbf{W} = \{\mathbf{w}_i\} = \{f_i(\mathbf{Z})\}$ denotes a latent space of item property matrix Y_i and personal characteristics matrix U_k , respectively, where $i = 1, \dots, p$ and $k = 1, \dots, n$.



In DLSJM, we assume the two sets of multiple view networks \mathbf{Y} and \mathbf{U} are conditionally independent given the latent space \mathbf{Z} . The DLSJM can

then be specified as

$$(2.8) \quad \begin{aligned} P(\mathbf{Y}, \mathbf{U} \mid \mathbf{Z}, \boldsymbol{\beta}, \boldsymbol{\theta}) &= \prod_{i=1}^p P(Y_i \mid \mathbf{Z}, \beta_i) \prod_{k=1}^n P(U_k \mid \mathbf{Z}, \theta_k) \\ &= \prod_{i=1}^p \prod_{k \neq l} \frac{\exp(\beta_i - \|\mathbf{z}_k - \mathbf{z}_l\|)^{y_i, kl}}{1 + \exp(\beta_i - \|\mathbf{z}_k - \mathbf{z}_l\|)} \prod_{k=1}^n \prod_{i \neq j} \frac{\exp(\theta_k - \|f_i(\mathbf{z}) - f_j(\mathbf{z})\|)^{u_k, ij}}{1 + \exp(\theta_k - \|f_i(\mathbf{z}) - f_j(\mathbf{z})\|)}, \end{aligned}$$

where the interpretations of the item intercept parameter β_i and the person intercept parameter θ_k stay the same as in Equations (2.3) and (2.5). With the prior distributions, $p(\beta_i) \sim N(0, \sigma_\beta^2)$, $p(\theta_k) \sim N(0, \sigma_\theta^2)$, and $\mathbf{z}_k \sim N(0, \sigma_z^2 I_D)$ with fixed σ_β^2 , σ_θ^2 , σ_z^2 , the posterior distribution of $\boldsymbol{\beta}$, $\boldsymbol{\theta}$ and \mathbf{z}_k can be specified as follows:

$$(2.9) \quad \begin{aligned} \pi(\beta_i \mid Y_i, \mathbf{Z}) &\propto \pi(\beta_i) \prod_{k \neq l} \frac{\exp(\beta_i - \|\mathbf{z}_k - \mathbf{z}_l\|)^{y_i, kl}}{1 + \exp(\beta_i - \|\mathbf{z}_k - \mathbf{z}_l\|)}, \\ \pi(\theta_k \mid U_k, \mathbf{Z}) &\propto \pi(\theta_k) \prod_{i \neq j} \frac{\exp(\theta_k - \|f_i(\mathbf{z}) - f_j(\mathbf{z})\|)^{u_k, ij}}{1 + \exp(\theta_k - \|f_i(\mathbf{z}) - f_j(\mathbf{z})\|)}, \\ \pi(\mathbf{z}_k \mid \mathbf{Y}, \mathbf{U}, \boldsymbol{\beta}, \boldsymbol{\theta}) &\propto \pi(\mathbf{z}_k) \prod_{i=1}^p P(Y_i \mid \mathbf{z}_k, \beta_i) \prod_{k=1}^n P(U_k \mid f_i(\mathbf{z}_k), \theta_k). \end{aligned}$$

3. Markov Chain Monte Carlo Estimation. To estimate the model parameters $\boldsymbol{\beta}$, $\boldsymbol{\theta}$, and the latent positions \mathbf{Z}_k , we apply a standard Bayesian approach with Metropolis-Hasting algorithm (Hoff, Raftery and Handcock, 2002; Handcock, Raftery and Tantrum, 2007; Krivitsky et al., 2009; Raftery et al., 2012; Rastelli, Friel and Raftery, 2015). One iteration of the Markov chain Monte Carlo (MCMC) sampler for DLSJM can be described as follows:

1. For each k in a random order, propose a value \mathbf{z}'_k from the proposal distribution $\varphi_{1k}(\cdot)$ and accept with probability

$$r_z(z'_k, z_k^{(t)}) = \frac{\pi(\mathbf{z}'_k \mid \mathbf{z}_{-k}, \mathbf{Y}, \mathbf{U}, \boldsymbol{\beta}, \boldsymbol{\theta})}{\pi(\mathbf{z}_k^{(t)} \mid \mathbf{z}_{-k}, \mathbf{Y}, \mathbf{U}, \boldsymbol{\beta}, \boldsymbol{\theta})}$$

where \mathbf{z}_{-k} are all components of \mathbf{Z} except \mathbf{z}_k .

2. Propose β'_i from the proposal distribution $\varphi_2(\cdot)$ and accept with probability

$$r_\beta(\beta'_i, \beta_i^{(t)}) = \frac{\pi(\beta'_i \mid Y_i, \mathbf{Z})}{\pi(\beta_i^{(t)} \mid Y_i, \mathbf{Z})}$$

3. Propose θ'_k from the proposal distribution $\varphi_3(\cdot)$ and accept with probability

$$r_\theta(\theta'_k, \theta_k^{(t)}) = \frac{\pi(\theta'_k | U_k, \mathbf{Z})}{\pi(\theta_k^{(t)} | U_k, \mathbf{Z})}$$

The MCMC sampler for DLSJM is time-consuming, especially for large datasets for the following reasons (Raftery et al., 2012): (1) Updating \mathbf{Z} requires calculating $n \times (n - 1) \times (p - 1)$ terms of the log-likelihood. (2) Updating of $\boldsymbol{\beta}$ and $\boldsymbol{\theta}$ requires calculating all $p \times \binom{n}{2}$ and $n \times \binom{p}{2}$ terms of the log-likelihood. Both (1) and (2) updates need at least $O(n^2p)$ calculations at each iteration of the MCMC algorithm. That is, the computational cost of DLSJM becomes quickly expensive as the number of respondents and the number of items increase in the data.

To alleviate computational burden of DLSJM, we utilize a parallel computing technique (OpenMP) in the MCMC computation. Alternatively, the computational complexity can be reduced by approximating the log-likelihood with a case-control approximate likelihood (Raftery et al., 2012) or by estimating the parameters based on the variational approximation with EM algorithm (Gollini and Murphy, 2016).

To apply the described algorithm to DLSJM, we determine the proposal distribution $\varphi_1(\cdot)$ for \mathbf{z}_k based on the degree of node k . When $y_{kl} = 1$, the Euclidean distance between the latent spaces of nodes k and l is likely to remain small. Hence, an edge when $y_{kl} = 1$ serves as a regulation for determining the latent spaces of \mathbf{z}_k and \mathbf{z}_l . This means that if node k is highly-connected, the latent space \mathbf{z}_k is not far from the prior mean of \mathbf{Z} (the origin in the present setting). This makes an MCMC update of \mathbf{z}_k highly unlikely. If node k has no connections with other nodes, an MCMC chain for \mathbf{z}_k explores all possible Euclidean latent spaces due to the lack of regulations. In this case, the estimates of \mathbf{z}_k may be unreliable. Therefore, for an efficient mixing of the MCMC chain, we will apply a different jumping rule for a proposal distribution based on the degree of a node, for instance, applying a small jumping rule for heavily-connected nodes, while a large jumping rule for lightly-connected nodes.

As aforementioned, due to the invariance property of latent spaces, we will utilize distance measures between pairs of respondents' and items' latent spaces to check convergence of the MCMC algorithm. The convergence of the distance measures for DLSJM is guaranteed, regardless of the fact that item latent spaces are a function of the respondent latent spaces, because the distance measures are included in the MCMC acceptance ratio. Trace plots in Section C in the supplement materials show the convergence of distance measures for item latent spaces for all of our numerical examples.

4. Illustration. We will first illustrate how our proposed methodology works based on a small data example. The data came from a study of patients admitted to an emergency room suffering from chest pain (Galen and Gambino, 1975). Each of four indicators (history, EKG (inverted Q-wave), CPK and LDH blood tests) was scored as either indicating (1) or not indicating (0) myocardial infarction (MI; commonly known as heart attack). It has been reported that the data did not fit well with complete independence or quasi-independence models (Rindskopf and Rindskopf, 1986), implying that some local dependence does exist in the data.

TABLE 2
The item intercept parameter estimates (β) and their 95% HPD interval for the MI symptom data.

Item	β	95% HPD Interval (β)
History	0.5261	(0.3914, 0.6616)
EKG	0.9604	(0.8290, 1.0943)
CPK	2.9602	(2.8026, 3.1097)
LDH	1.7659	(1.6270, 1.9015)

With this example, we will describe how to interpret all estimated model parameters (item intercept parameters, person intercept parameters, estimated distance measures among items and among persons) and to illustrate how the item and person dependence structures can be visualized in latent spaces.

TABLE 3
Five number summary of the person intercept parameter estimates (θ) categorized by the total scores for the MI symptom data (minimum, first quartile, median, third quartile, maximum).

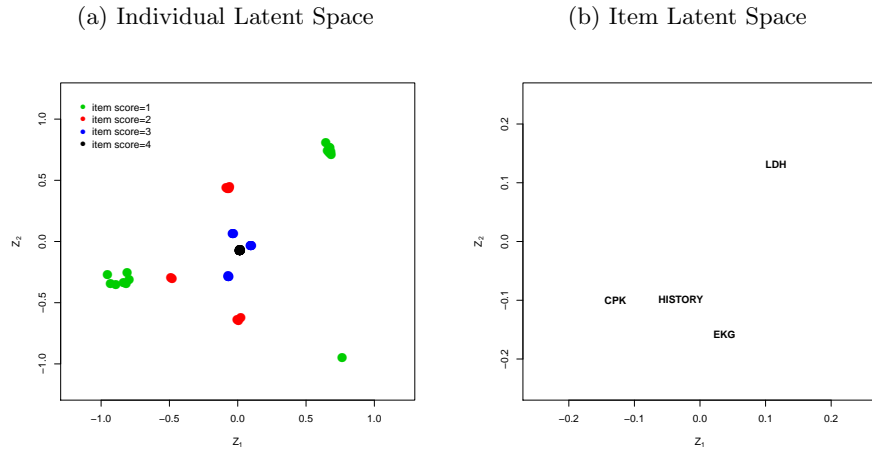
Item Score	min	25%	median	75%	max
0	-2.8029	-2.7596	-2.7524	-2.7323	-2.7169
1	-2.7766	-2.7637	-2.7584	-2.7492	-2.7284
2	-1.1525	-1.1507	-1.1434	-1.1401	-1.1232
3	0.4932	0.4999	0.5071	0.5147	0.5309
4	3.4680	3.4881	3.4958	3.5016	3.5157

MCMC was implemented as described in Section 3. The MCMC run consisted of 55,000 iterations with the first 5,000 iterations being discarded as a burn-in process. From the remaining 50,000 iterations, 5,000 samples were collected at a time space of 10 iterations. A 2-dimensional Euclidean latent space was used for this example. To prevent the separation problem of a logistic regression, we fix $\sigma_\theta = \sigma_\beta = 2.5$. To prevent the overestimation issue, we fix $\sigma_z = 2$. A jumping rule was set to 0.1 for $\varphi_2(\cdot)$ and to 3.0 for $\varphi_3(\cdot)$. For $\varphi_1(\cdot)$, five different jumping rules were used based on the degree of a

node (2.0, 1.0, 0.75, 0.5, and 0.2).

Table 2 displays the estimates of the item intercept parameters (β) and their 95% HPD intervals for the MI symptom data. The result suggests that the two blood tests (CPK and LDH) have larger β estimates, meaning that these two indicators are more likely to be endorsed by the patients than the other items regardless of their different possibilities of heart attack. The History indicator shows the smallest β estimates among the four items, meaning that this item is the least likely to be endorsed by many patients.

FIG 3. Visualization of the DLSJM for the MI symptom data: (a) A latent space for patients grouped by total scores; and (b) An illustrations of an item latent space.



To summarize the estimates of the person intercept parameter (θ), we grouped all patients in the data by their total scores and made a five number summary of the θ estimates per group. See Table 3. The result suggests that the θ estimates tend to increase as more indicators are endorsed (or the total score increases). Note that there seems little difference in the θ estimates between the total scores 0 and 1. This is because the item network view is constructed with the multiplication of an item pair (items i and j) for respondent k . Hence, when the total score is 1, the resulting adjacency matrix becomes an empty matrix, which is the same as when the total score is 0.

Figure 3(a) visualizes a patient latent space. The positions of all patients who have non-zero total scores are displayed and colored by their total scores (black, blue, red, and green colors represent the total score of 4, 3, 2, and 1, respectively). It is clear from Figure 3(a) that the latent spaces for the patients whose total score is 4 (maximum score) are not far from the origin

(prior mean of \mathbf{Z}), whereas the latent spaces for the patients whose total score is 1 (minimum non-zero total score) are located the farthest from the origin. This affirms our earlier claim that different jumping rules should be used for \mathbf{Z} based on the respondents' total scores.

TABLE 4
Relative distances between item latent spaces for the MI symptom data.

	History	EKG	CPK	LDH
History	-	0.2876	0.2920	0.7958
EKG	0.2876	-	0.5331	0.8874
CPK	0.2920	0.5331	-	1.0000
LDH	0.7958	0.8874	1.0000	-

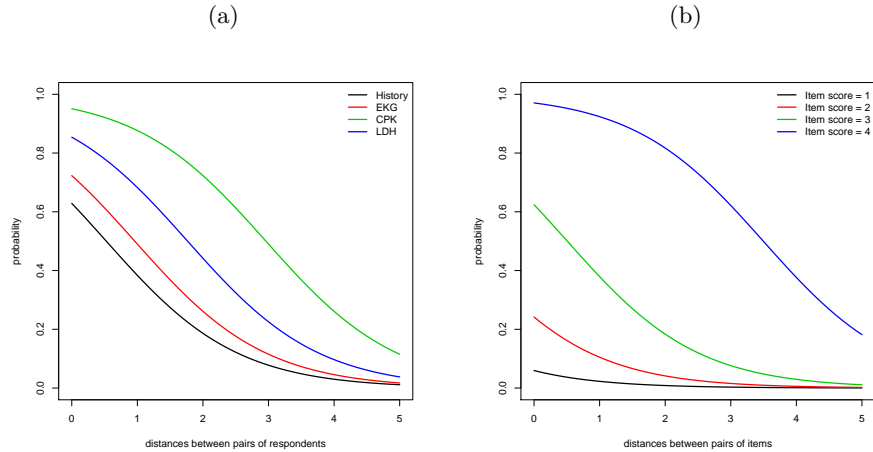
As a measure of item local dependence, we suggest to use a relative distance r_{ij} between the latent spaces of items i and j , which is defined as

$$r_{ij} = \frac{d_{ij}}{\max_{v_i, j} d_{ij}} = \frac{\|f_i(\mathbf{z}) - f_j(\mathbf{z})\|}{\max_{v_i, j} \|f_i(\mathbf{z}) - f_j(\mathbf{z})\|}.$$

By mapping an absolute distance d_{ij} into a relative $[0, 1]$ space (r_{ij}), we can easily detect item local dependence; as r_{ij} becomes close to 0, local dependence between the item pair gets larger. Table 4 shows the relative distance measures among the four indicators. The result suggests that local dependence appears to exist among History, EKG, and CPK indicators. This local dependence structure is also observed in the item latent space displayed in Figure 3(b).

Finally, we display the correct response probabilities for the MI symptom data in Figure 4. Figure 4(a) presents the probability of a pair of respondents endorsing 'Yes' to each item by the latent space distance between the respondent pair; and Figure 4(b) shows the probability of a pair of items being endorsed as 'Yes' by patient groups (who have the same total scores) by the latent space distance between the item pair. Note that these two plots are different from the item and person characteristic curves used for regular IRT models. The key difference is that the latent space distances between the pair of respondents (a) and the latent space distances between the pair of items (b) are used on the x-axis. In both plots, as the latent space distances increase (or the characteristics of the pair of persons and the pair of items become more different from each other), the correct response probabilities decrease. The latent space distances range from 0 to 5 in both plots. With the MI symptom data, the maximum item latent space distance was 1.04 (Figure 4(b)), while the maximum person latent space distance was 5.34 (Figure 4(a)). Note that the item intercept parameter (β) can be obtained

FIG 4. *Correct Response Probabilities for the MI symptom data: (a) the probability of a pair of respondents endorsing ‘Yes’ to each item by the latent space distance between the respondent pair; and (b) the probability of a pair of items being endorsed as ‘Yes’ by patient groups (who have the same total scores) by the latent space distance between the item pair.*



after inverse logit transforming the correct response probability when the person latent space distance is 0. Similarly, the person intercept parameter (θ) is obtained after inverse logit transforming the correct response probability when the item latent space distance is 0.

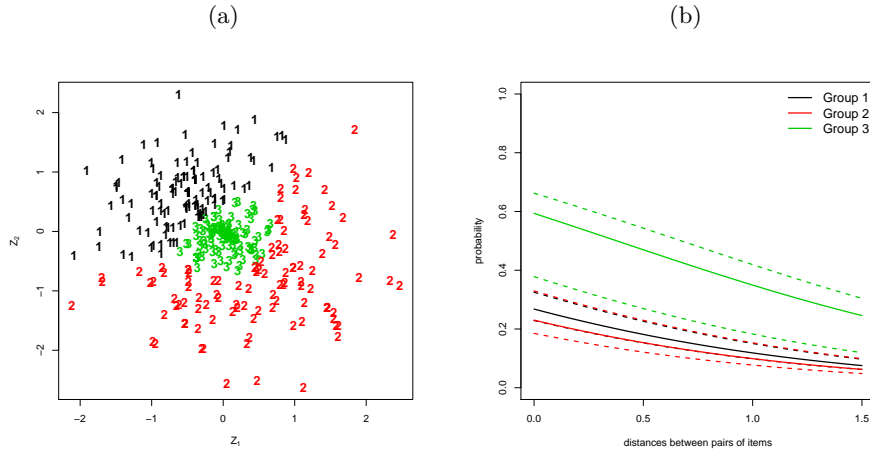
5. Application to DRV Data. We return to the DRV test data introduced in Section 1. The DRV data contain binary responses to 24 items for 418 students. The test items were developed based on three theoretical design factors. Hence, there is likely to be a strong dependence structure among the items that share similar test design features, although the details of the empirical item dependence structure are unknown. Moreover, the data include students from different cognitive developmental stages and in each developmental stage, there is an additional dependence structure among students due to responses pattern similarities across the test items. Therefore, we applied our proposed DLSJM to analyze the DRV test items.

Similar to the illustrative example in Section 4, the MCMC run consisted of 55,000 iterations with the first 5,000 iterations being discarded as a burn-in process. From the remaining 50,000 iterations, 5,000 samples were collected at a time space of 10 iterations. A 2-dimensional Euclidean latent space was used for the DRV data. We fix $\sigma_\theta = \sigma_\beta = 2.5$ and fix $\sigma_z = 2$. A jumping rule was set to 0.1 for $\varphi_2(\cdot)$ and to 3.0 for $\varphi_3(\cdot)$. We set different

jumping rules for $\varphi_1(\cdot)$ and a description of the rules were provided in the supplementary material.

In Tables 1, 2, and 3 of the supplementary material, we provided: (1) the item intercept parameters (β) and their 95% HPD intervals, (2) a five number summary of the person intercept parameter (θ) grouped by students' total scores, and (3) the relative distance measures among the 24 items.

FIG 5. (a) A latent space for students with spectral clustering results (with 3 clusters); and (b) Corrected response probabilities by three student clusters



Here we focus on examining the item and person dependence structures of the DRV data. To have a more clear visualization of the dependence structures, we additionally applied a spectral clustering technique (Ng, Jordan and Weiss, 2002; von Luxburg, 2007) that utilizes the spectrum (eigenvalues) of the similarity matrix of the data for clustering and that is implemented with the `specClust` function in the `kknn` R package (Hechenbichler and Schliep, 2004). In our analysis, we used the negative exponential of the estimated distance matrices between pairs of item latent spaces and between pairs of person latent spaces as the similarity matrices for item and person clustering, respectively. We used k -nearest neighbor graphs, while selecting k such that the explanatory power of clustering is maximized. For the person clustering, $k = \lfloor .21 \times n \rfloor$ was chosen with 88.5% variance explained (where n is the total number of persons). For the item clustering, $k = 2$ was chosen with 97.8% variance explained.

Figure 5(a) shows the student clustering results in the two-dimensional latent space. To visualize the dependence structure of students' latent space, we chose three clusters based on the reasoning that there would be three stu-

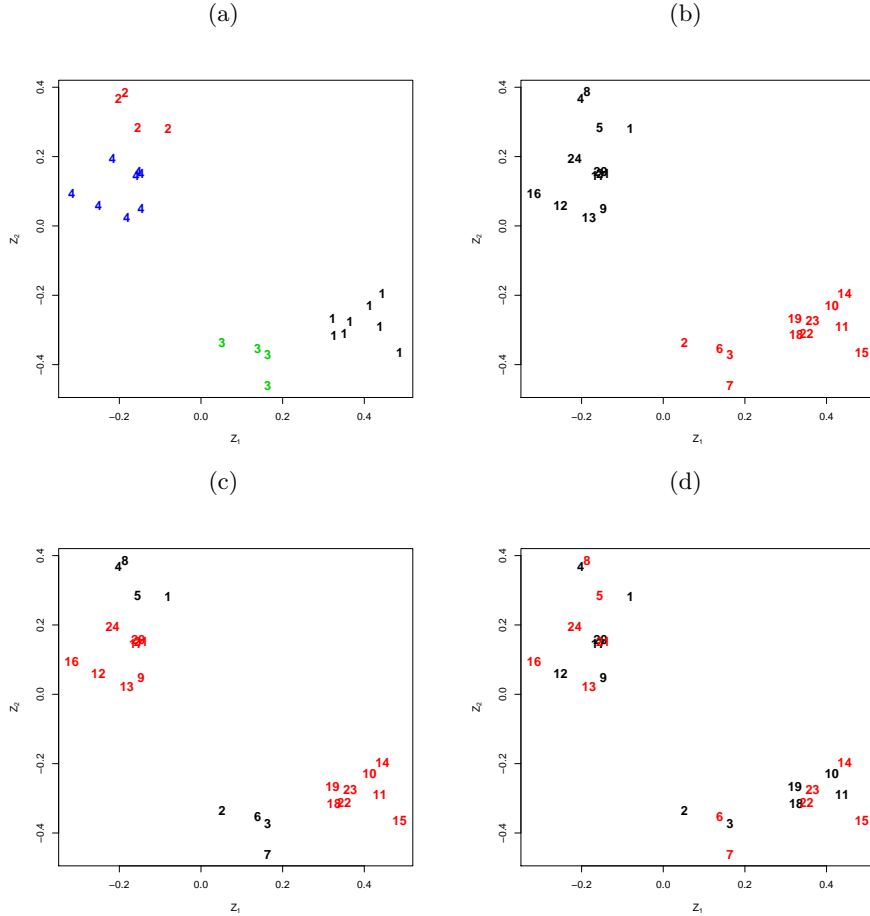
dent groups that correspond to the concrete-operational stage, the formal-operational stage, and the transition between the stages. Specifically, Cluster 3 students tend to be located around the origin (prior mean) of the latent space, meaning that those students provided correct answers more often than students in the other clusters. This implies that students in Cluster 3 are likely to belong to the formal-operational stage. Clusters 1 and 2 are clearly differentiated from each other and from Cluster 3. However, solely based on their locations in the latent space, it is hard to identify which cluster corresponds either to the concrete-operational stage or to the transition period. Hence, we checked the response patterns of the students in Clusters 1 and 2; the results showed that students in Cluster 1 tended to correctly answer concrete items (MT/MP) but fail to give correct answers to most logical fallacy items (NA/AC). Cluster 2 students showed the opposite tendency; they tended to correctly answer fallacy items (NA/AC), while sometimes giving incorrect answers to concrete items. Based on these item response patterns, we concluded that students in Cluster 1 correspond to the concrete-operational stage, while Cluster 2 students likely correspond to the transition between the concrete- to formal-operational stage.

Figure 5(b) displays the probability of a pair of items being correctly answered by the student clusters (based on the spectral clustering results) as a function of the latent space distance between the item pairs. A solid line represents the inverse logit of the mean θ value for each group. Lower and upper dotted lines around each solid line indicate the inverse logit of the 25% and 75% quantile of θ values for each group. Black lines correspond to Cluster 1, red lines to Cluster 2, and green lines to Cluster 3. As we can see, Cluster 3 students show clearly higher correct responses probabilities than students in the other clusters. This confirms our conclusion that Cluster 3 corresponds to the formal-operational group. Clusters 1 and 2 do not show distinctive differences in their correct response probabilities.

Figure 6(a) displays the item clustering results in the two-dimensional latent space. We chose four clusters to describe the item dependence structure, as shown in the item latent space plot. Note that in contrast to the person case, item dependence structures can be easily visualized because the item latent space W is assumed to be a function of the person latent space Z . Cluster 1 consists of items which belong to a NA/AC group in Type of inference and a AB/CF group in Content of the conditional. Cluster 2 includes items that belong to a MP/MT group in Type of inference and a CO group in Content of the conditional. Cluster 3 contains items that belong to a MP/MT group in Type of inference and a AB/CF group in Content of the conditional. Cluster 4 have items that belong to a NA/AC group in

Type of inference and a CO group in Content of the conditional.

FIG 6. *Item latent spaces: (a) a latent space with spectral clustering results (with 4 clusters), (b) a latent space for items color-coded by type of inference, (c) a latent space for items color-coded by contents of the conditional, and (d) a latent space for items color-coded by presentation of antecedents.*



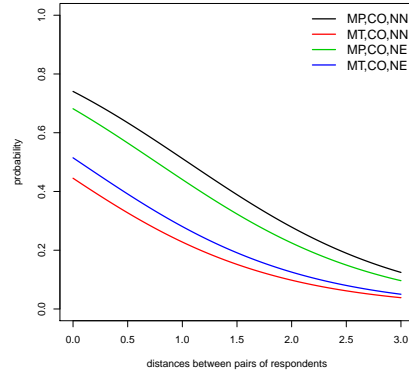
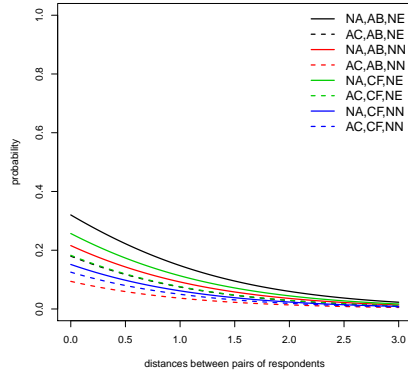
In Figures 6(b) to (d), we displayed three item latent spaces where items are color-coded based on each of the three test design factors. In Figure 6(b) that uses Type of inference, the red items correspond to the NA/AC item group, while the black items indicate the MP/MT item group. In Figure 6(c) that uses Content of the conditional, the red items correspond to the AB/CF item group, while the black items indicate the CO item group. In Figure 6(d) that is based on Presentation of antecedents, the red items correspond to the NE item group, while the black items indicate the NN item group.

As we can see in Figure 6(d), the two Presentation of antecedents groups are not clearly differentiated in the item latent space. This means that the DRV test's item dependence structure is not related to the Presentation of antecedents design factor.

FIG 7. Corrected response probabilities by item clusters

(a) Cluster 1

(b) Cluster 2



(a) Cluster 3

(b) Cluster 4

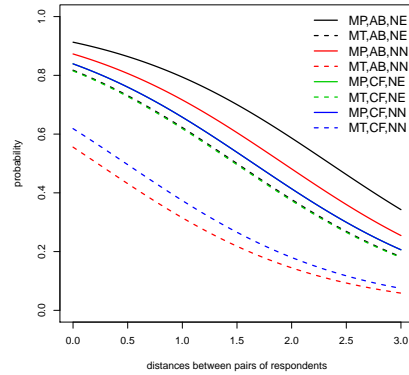
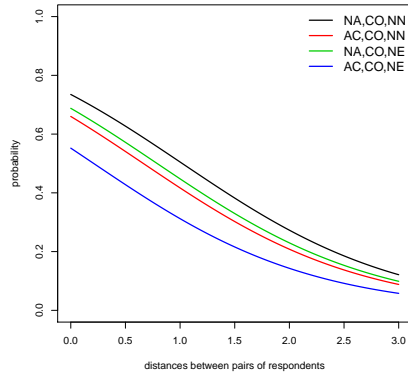


Figure 7 displays the probability of a pair of students correctly answering four item clusters (based on the spectral clustering results) as a function of the latent space distance between the student pairs. This figure shows that (1) NN items are generally easier than NE items, (2) In the case of CO, the correct response probabilities are in the order of $MP \approx NA > AC > MT$, and (3) In the case of AB/CF, the correct response probabilities are in the order of $MP > MT \gg NA > AC$. That is, the difficulty order of the type of

inference item groups is not consistent across the contents of the conditional groups due to the items' dependence structure.

6. Discussion. The current study was motivated by the need to analyze complex cognitive test data that simultaneously present unknown local item dependence and person dependence. Current item response modeling approaches cannot properly handle such cases. In this study, we proposed an innovative method that can analyze unknown item and person dependence structures as item network views and person network views, respectively.

Specifically, we first construct two collections of person network views and item network views to estimate the item intercept and person intercept parameters, respectively. To combine the multiple network views, we apply respective latent space joint models to the person network views and the item network views. The resulting, two latent space joint models for the person network and item network views are integrated by assuming that the latent space for an item is a function of latent spaces for all people. This way, a combined latent space joint model, or so-called doubly latent space joint model (DLSJM) can be constructed and estimated with a Bayesian approach.

Note that the proposed model provides the estimates of the item intercept parameters as well as the person intercept parameters which are similar to the item easiness parameters and the person latent trait parameters in regular IRT models. As discussed in the paper, the specific interpretation of the parameters is not equivalent to the regular IRT model case. However, one can still use the item intercept parameter estimates to compare the overall easiness level of individual items and further utilize the person intercept parameter estimates to examine person trait differences.

To clearly show the dependence structures, we also proposed to apply spectral clustering (which is based on similarity measures) to the item and person latent spaces as a post-analysis. The clustering results from the DRV data analysis showed that there were interactions between two design factors, the type of inference and the content of the conditional. Additionally, the students were clustered into three groups that correspond to the concrete-operational stage, the formal-operational stage, and the transition between the stages.

In literature, a network modeling approach has been applied to item response data based on an Ising model, for the purpose of visualizing interactions among items (van Borkulo et al., 2014). However, the key difference is that their approach still requires the local item independence assumption, whereas our approach does not. By assuming local (or conditional) inde-

pendence, [van Borkulo et al. \(2014\)](#) intended to avoid the computational difficulty that arises from doubly-intractable normalizing constants of the Ising model. However, assuming the conditional independence and estimating interaction parameters of the Ising model using a maximum pseudo-likelihood estimator (MPLE; [Besag, 1974](#)) is invalid because it overlooks the dependence structure embedded in the Ising model (e.g., [Jin and Liang, 2013](#); [Liang et al., 2016](#)). To accurately estimate Ising model parameters without the conditional independence assumption, advanced computational algorithms are needed, for example, MCMC MLE ([Geyer and Thompson, 1992](#); [Hunter and Handcock, 2006](#)), stochastic approximation MCMC methods ([Jin and Liang, 2013](#)), M oller and exchange algorithms ([M oller et al., 2006](#); [Murray, Ghahramani and MacKay, 2006](#)), adaptive exchange sampler ([Liang et al., 2016](#)), and Russian roulette sampling algorithm ([Lyne et al., 2013](#)).

Our proposed approach provides a new practical tool for item response analysis that can be used regardless of the presence of locally dependent items and persons. Our method can also be to create statistical indices to evaluate local dependence among items and among people, which can be useful during test construction, test validation, and scoring purposes. In addition, we will extend the proposed model with observed person-level and item-level covariates (e.g., characteristics of pairs of persons and pairs of items, respectively) to explain differences in the item intercept parameters and the person intercept parameters. For instance, by including a subjects' group membership (e.g., treatment vs. control groups) as person-level covariates, we can investigate whether there are differences in the item and person intercept parameters between the two groups. Further, we can expand the proposed model in several other ways, e.g., to handle data with missing observations, longitudinal data, multidimensional item designs, and hierarchical person structures.

References.

- BESAG, J. (1974). Spatial interaction and the statistical analysis of lattice systems. *Journal of the Royal Statistical Society. Series B* **36** 192-236.
- BREIGER, R. L., BOORMAN, S. A. and ARABIE, P. (1975). An algorithm for clustering relational data, with applications to social network analysis and comparison with multidimensional scaling. *Journal of Mathematical Psychology* **12** 328-383.
- BYRNES, J. P. and OVERTON, W. F. (1986). Reasoning about certainty and uncertainty in concrete, causal, and propositional context. *Developmental Psychology* **22** 793-799.
- CHEN, W. H. and THISSEN, D. (1997). Local dependence indexes for item pairs using item response theory. *Journal of Educational and Behavioral Statistics* **22** 265-289.
- DAVISON, M. L. (1983). *Multidimensional scaling*. Wiley, New York.

- DRANEY, K., WILSON, M., GLUCK, J. and SPIEL, C. (2007). Mixture models in a developmental context. In *Latent variable mixture models* (R. Hancock and K. M. Samuelson, eds.) 199-216. Information Age, Charlotte, NC.
- EVANS, J. S. B. T., NEWSTEAD, S. E. and BYRNE, R. M. J. (1993). *Human reasoning: The psychology of deduction*. Erlbaum, Mahwah, NJ.
- FOX, J. P. and GLAS, C. A. W. (2001). Bayesian estimation of a multilevel IRT model using Gibbs sampling. *Psychometrika* **66** 271-288.
- GALEN, R. S. and GAMBINO, S. R. (1975). *Beyond normality: The predictive value and efficiency of medical diagnoses*. New York: John Wiley & Sons, Inc.
- GEYER, C. J. and THOMPSON, E. A. (1992). Constrained Monte Carlo Maximum Likelihood for Dependent Data. *Journal of the Royal Statistical Society, Series B* **54** 657-699.
- GOLLINI, I. and MURPHY, T. B. (2016). Joint modeling of multiple network views. *Journal of Computational and Graphical Statistics* **25** 246-265.
- HANDCOCK, M. S., RAFTERY, A. E. and TANTRUM, J. M. (2007). Model-based clustering for social network. *Journal of the Royal Statistical Society, Series A* **170** 301-354.
- HECHENBICHLER, K. and SCHLIEP, K. P. (2004). Weighted k-Nearest-Neighbor Techniques and Ordinal Classification Technical Report No. 399, Ludwig-Maximilians University Munich.
- HOFF, P., RAFTERY, A. and HANDCOCK, M. (2002). Latent space approaches to social network analysis. *Journal of the American Statistical Association* **97** 1090-1098.
- HUNTER, D. R. and HANDCOCK, M. S. (2006). Inference in curved exponential family models for networks. *Journal of Computational and Graphical Statistics* **15** 565-583.
- JANVEAU-BRENNAN, G. and MARKOVITS, H. (1999). The development of reasoning with causal conditionals. *Developmental Psychology* **35** 904-911.
- JIN, I. H. and LIANG, F. (2013). Fitting social network models using varying truncation stochastic approximation MCMC algorithm. *Journal of Computational and Graphical Statistics* **22** 927-952.
- KRIVITSKY, P. N., HANDCOCK, M. S., RAFTERY, A. E. and HOFF, P. D. (2009). Representing degree distributions, clustering, and homophily in social networks with latent cluster random network models. *Social Networks* **31** 204-213.
- LIANG, F., JIN, I. H., SONG, Q. and LIU, J. S. (2016). An adaptive exchange algorithm for sampling from distributions with intractable normalizing constants. *Journal of the American Statistical Association* **111** 377-393.
- LIU, Y. and MAYDEU-OLIVARES, A. (2012). Local dependence diagnostics in IRT modeling of binary data. *Educational and Psychological Measurement* **73** 254-274.
- LYNE, A., GIROLAMI, M., ATCHADE, Y., STRATHMANN, H. and SIMPSON, D. (2013). Playing Russian roulette with intractable likelihoods. arXiv:1306.4032v4.
- MARKOVITS, H., FLEURY, M. L., QUINN, S. and VENET, M. (1998). The development of conditional reasoning and the structure of semantic memory. *Child Development* **69** 742-755.
- MÓLLER, J., PETTITT, A. N., REEVES, R. W. and BERTHELSEN, K. K. (2006). An efficient Markov chain Monte Carlo method for distributions with intractable normalising constants. *Biometrika* **93** 451-459.
- MUCHA, P. J., RICHARDSON, T., MACON, K., PORTER, M. A. and ONNELA, J. P. (2010). Community structure in time-dependent, multiscale, and multiplex networks. *Science* **328** 876-878.
- MURRAY, I., GHAHRAMANI, Z. and MACKAY, D. J. (2006). MCMC for doubly-intractable distributions. In *Proceedings of 22nd Annual Conference on Uncertainty in Artificial Intelligence (UAI)* (R. DECHTER and T. S. RICHARDSON, eds.) 359-366. AUAI Press, Cambridge, MA.

- NG, A., JORDAN, M. and WEISS, Y. (2002). On spectral clustering: analysis and an algorithm. In *Advances in Neural Information Processing Systems* (T. DIETTERICH, S. BECKER and Z. GHAHRAMANI, eds.) **14** 849-856. MIT Press, Cambridge, MA.
- OH, M. S. and RAFTERY, A. E. (2001). Bayesian multidimensional scaling and choice of dimension. *Journal of the American Statistical Association* **96** 1031-1044.
- OVERTON, W. F. (1985). Scientific methodologies and the competence- moderator performance issue. In *Moderators of competence* (E. D. Neimark, R. de Lisi and J. L. Newman, eds.) 15-41. Erlbaum, Hillsdale.
- PIAGET, J. (1971). *Biology and knowledge*. Chicago, University of Chicago Press.
- RAFTERY, A. E., NIU, X., HOFF, P. D. and YEUNG, K. Y. (2012). Fast inference for the latent space network model using a case-control approximate likelihood. *Journal of Computational and Graphical Statistics* **21** 909-919.
- RASTELLI, R., FRIEL, N. and RAFTERY, A. E. (2015). Properties of latent variable network models. arXiv:1506.07806.
- RINDSKOPF, D. and RINDSKOPF, W. (1986). The value of latent class analysis in medical diagnosis. *Statistics in Medicine* **5** 21-27.
- ROBERGE, J. J. and MASON, E. J. (1978). Effects of negation on adolescents' class and conditional reasoning abilities. *The Journal of General Psychology* **98** 187-195.
- SHORTREED, S., HANDCOCK, M. S. and HOFF, P. (2006). Positional estimation within a latent space model for networks. *Methodology* **2** 24-33.
- SPIEL, C., GLUCK, J. and GOSSLER, H. (2001). Stability and change of unidimensionality: The sample case of deductive reasoning. *Journal of Adolescent Research* **16** 150-168.
- SPIEL, C. and GLUCK, J. (2008). A model based test of competence profile and competence level in deductive reasoning. In *Assessment of competencies in educational contexts: State of the art and future prospects* (J. Hartig, E. Klieme and D. Leutner, eds.) 41-60. Hogrefe, Gottingen.
- VAN BORKULO, C. D., BORSBOOM, D., EPSKAMP, S., BLANKEN, T. F., BOSCHLOO, L., SCHOEVEERS, R. A. and WALDROP, L. J. (2014). A new method for constructing networks from binary data. *Scientific Reports* **4** 1-10.
- VON LUXBURG, U. (2007). A tutorial on spectral clustering. *Statistics and Computing* **17** 395-416.

DEPARTMENT OF APPLIED AND
COMPUTATIONAL MATHEMATICS AND STATISTICS
UNIVERSITY OF NOTRE DAME
NOTRE DAME, INDIANA, 46556, USA
E-MAIL: ijin@nd.edu

GRADUATE SCHOOL OF EDUCATION
AND INFORMATION STUDIES
UNIVERSITY OF CALIFORNIA, LOS ANGELES
LOS ANGELES, CA, 90095, USA
E-MAIL: mjjeon@ucla.edu